Computers and Structures 290 (2024) 107193

Contents lists available at ScienceDirect

Computers and Structures

journal homepage: www.elsevier.com/locate/compstruc

Buckling of stretched strips - reconsidered and extended

Franz G. Rammerstorfer

Vienna University of Technology (TU Wien), Inst. of Lightweight Design and Struct. Biomechechanics, Vienna, Austria

ARTICLE INFO

Keywords:
Structural stability
Buckling
Stretched strip
Auxetics
Mode transitions

ABSTRACT

The paper "Buckling of stretched strips" [1], published in the year 2000, seemed to deal with a rather specific problem of buckling of thin structures. Nevertheless, it aroused quite broad interest and prompted a considerable series of further treatments. Deeper theoretical considerations and advanced applications have been published. Various specific aspects of this type of problem have been addressed in these papers. However, a general and systematic consideration of how and to what extent the Poisson's ratio affects the critical stretch of strips of different length to width ratios, L/B, was lacking. Accomplishing this task is the focus of this paper. Given the increasing use of auxetics, strips made from such materials are also being investigated. In addition, the occurrence of previously undiscovered mode transitions is shown. All results are presented in dimensionless form, which allows for fairly general usage.

1. Introduction

Strips are geometrically most simple. However, even if the simplest material model, i.e., linear elastic, is used, a lot of strange behaviors can be observed. Therefore, strips are interesting objects also from the viewpoint of theoretical mechanics.

Buckling of thin structures under tensile loading has been considered already for long. First papers dealing with this phenomenon have considered circular plates, stretched along a diameter, such as treated as a special case in [2], later on in [3] and recently in more detail in [4]. Square plates, stretched along a diagonal have also been considered long ago, see [5]. In [6] wrinkling of simply supported rectangular plates under parabolic distribution of tensile forces at two opposite edges is considered. A further class of problems in this context is buckling of thin stretched plates with cracks or holes, see, e.g., [7], [8], [9] and [10]. An overview of these and much more papers dealing with buckling of tensile loaded structures can be found in [11].

Regarding buckling of stretched strips, after the appearance of the paper [1] a large number of projects have been started, dealing with the problem of instabilities in stretched strips under different aspects. Buckling of strips under global tension and residual stresses is considered in [12]. In 2002 a quite general paper appeared in the Journal "Nature", see [13]. In [14] the buckling problem of stretched strips has been treated analytically. Further analytical considerations as well as numerical computations regarding this problem area can be found in [15], [16], in [17], and in [18]. The fact that small variations in the loading conditions of stretched strips have a significant influence on the behavior is shown in [19], and in [20] as well as in [21] anisotropic strips are considered.

The disappearance of the wrinkles in the deep post-buckling regime has been studied theoretically in [22], [23] and experimentally in [24]. Flattening out of wrinkles in stretched strips with cracks or holes is treated in [11] and for strips made of hyperelastic material this phenomenon has been studied in [25] as well as, for polyethylene strips, in [26]. A detailed analysis of the disappearance of the wrinkles has been reported in [27]. In that paper it is expected that there exists a threshold for positive Poisson's ratios, below which no wrinkles occur. In [28] it is shown how the use of auxetics can reduce the height of the wrinkles in the post buckling regime.

Wrinkling of strips during a combination of stretching and twisting has been the topic in [29], [30], and [31]. Buckling phenomena in stretched strips consisting of a thin film on an elastic substrate have been presented, e.g., in [32], [33], and [34].

As argued in [11], in all the mentioned cases of buckling of thin elastic structures under tensile loading, areas are required, in which at least one of the principal in-plane normal stress components is compressive. Thus, one should not say buckling under tension, but buckling under tensile loading. Since in stretched strips these compressive stresses result from the Poisson's-effect suppressed at the clamped edges, it is clear that the Poisson's ratio of the material, the strip is made of, must have a significant influence on the critical tensile load. Previous investigations of the instability of stretched strips typically concerned strips made of materials with positive Poisson's ratios. However, strips made from auxetics are finding increasing use in various engineering and medical

E-mail address: ra@ilsb.tuwien.ac.at.

https://doi.org/10.1016/j.compstruc.2023.107193
Received 25 June 2023; Accepted 26 September 2023
Available online 10 October 2023

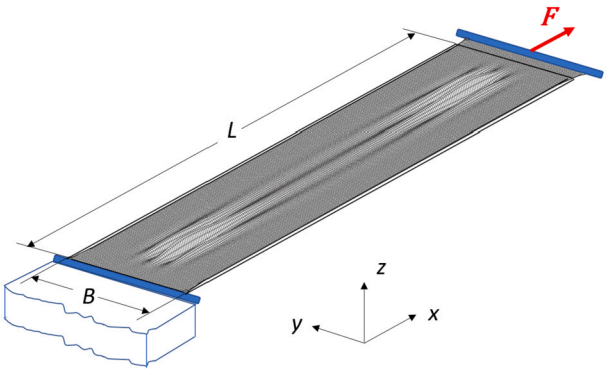

Fig. 1. The stretched strip. Both ends are clamped, one end is completely immovable, the other end is allowed to move just in direction x like a rigid beam.

applications and it has been observed that stretched strips of this material are also prone to wrinkling. It therefore seemed obvious to extend the investigations to negative Poisson's numbers.

There are many applications of thin, stretched strips in technical products or processes and in medical treatments where the strips must not wrinkle. Hence knowledge of the critical stretch, limiting the stability of the flat configuration, is required in such situations. If it can be assumed that the behavior of the problem is linear, the dimensionless representation of the critical stretch as a function of the aspect ratio L/B and the Poisson's number of the material from which the strips are made enables this critical state to be determined quickly.

Typical fields, in which this approach can be used, are stretched strips in general and their stability behavior in particular play an important role in flexible electronics, aerospace applications (e.g., deployable structures), in the behavior of endless belts for production, transmission and transport, in medical treatments, in chemistry, and in thin sheet production (leveling by stretching), just to mention a few fields of application. Some examples are presented below.

Typical situations, in which care must be taken to ensure that stretched strips do not wrinkle, occur, for example, when thin sheet strip is straightened in stretching lines, see [35]. Undesirable wrinkles appearing during conveying in processing lines are treated in [36]. Wrinkles in artificial skin are topic in [37]. As an example in the field of space structures, the reduction in the accuracy of deployable antennas due to stretch-induced fold formation is given in [38], and stability problems of stretched strips in batteries are, for instance, mentioned in [39]. In some applications, wrinkling is even a desirable phenomenon. An example, taken from cell biology, where this happens, is the appearance of wrinkles in the thin substrates on which natural cells are cultured. There, this wrinkling can be used as indicator of the traction forces exerted by cells during locomotion, see [40]. Although wrinkles in stretched flexible electronics should be avoided, this kind of instability can be used for determining the adhesion strength between the metallic film and the soft substrate, see [33].

2. Problem description and solution method

7

Consider a strip, made of homogeneous, isotropic, linear elastic material with Young's modulus E and Poisson's ratio ν. Both ends, i.e., the short edges are fully clamped, the left end is completely immovable, the right one is allowed to move as a "rigid" line in x-direction only and without any rotation. The two long edges are completely free, see Fig. 1.

As clearly described in [1] for positive Poisson's ratios, comparably small transversal compressive stresses, i.e., σ_{yy}, appear at some distance from the strip ends causing short wavelength buckling (wrinkling) if the stretch load is large enough. (By the way, since the transverse compressive stresses σ_{yy} are some orders of magnitudes smaller than the longitudinal stresses σ_{xx}, the principal stress axes in the considered region are nearly not inclined. Hence, it is acceptable to consider σ_{yy} as the buckling relevant principal normal stress component.)

As mentioned in the Introduction, some attempts have been made to obtain at least approximate solutions for the complex stress and stability problem. Since the focus of this paper lies on studying some principal figures of the buckling behavior when the Poisson's ratio is varied rather than on analytical derivations, in the present paper the finite element method is applied. The research code CARINA [41] is used, and the strip is discretized by 16-noded degenerated shell elements. Convergence studies were performed to validate the mesh.

Eigenvalue buckling analysis, based on Euler's buckling criterion, was used to determine the critical load, i.e., bifurcation or buckling load. According to Euler's static buckling criterion, at critical points (bifurcation or snap through points) the equilibrium state is not uniquely determined. In terms of a discretized system, this means that at a critical point the equation

$$\mathbf{K}^*\delta\mathbf{u} = \delta\mathbf{F} = \mathbf{0} \tag{1}$$

has at least one nontrivial solution

$$\delta\mathbf{u} \neq \mathbf{0}\ . \tag{2}$$

$\mathbf{K}^*$ is the tangent stiffness matrix at buckling load $\mathbf{F}^*$, including load and displacement dependent contributions according to a total Lagrangian formulation for geometric nonlinearities, and $\delta\mathbf{u}$ represents the nontrivial infinitely small deviation of the equilibrium state(s) in neighborhood of the trivial state, given by the displacement vector $\mathbf{u}$.

Assuming proportional loading, i.e., $\mathbf{F} = \lambda\mathbf{F}_{ref}$, with the reference loading $\mathbf{F}_{ref}$, for linear buckling analyses the following eigenvalue problem can be derived from Eq. (1):

$$(\mathbf{K}_0 + \eta_i\mathbf{K}_{lin}(\lambda = 1))\phi_i = \mathbf{0}\ , \tag{3}$$

where $\mathbf{K}_0$ is the stiffness matrix corresponding to the unloaded configuration, and

$$\mathbf{K}_{lin} = \mathbf{K}_{lin,u} + \mathbf{K}_{lin,g} \tag{4}$$

is the sum of the linearized initial displacement and initial stress stiffness matrices, determined with the displacement state calculated from $\mathbf{K}_0\mathbf{u} = \mathbf{F}_{ref}$.

For linear buckling analyses of thin structures, such as slender beams, thin plates and strips, for which the prebuckling deformations definitely play no role, $\mathbf{K}_{lin,u}$ can be neglected, leading to the classical eigenvalue problem

$$(\mathbf{K}_0 + \eta_i\mathbf{K}_{lin,g}(\lambda = 1))\phi_i = \mathbf{0}\ . \tag{5}$$

The eigenvalues η_i, $i = 1, 2, 3, ..$ lead to the critical loads $\mathbf{F}_i^* = \eta_i\mathbf{F}_{ref}$. Hence, the buckling load $\mathbf{F}^* = \mathbf{F}_1^* = \lambda^*\mathbf{F}_{ref}$ with $\lambda^* = \eta_1$. The eigenvectors ϕ_i, in conjunction with the elements' shape functions, render the buckling modes.

The eigenvalue solver used in CARINA determines the eigenvalues in the sequence $|\eta_1| \leq |\eta_2| \leq |\eta_3| \ldots$ In most buckling problems for tensile loaded structures, the critical load intensities are much larger than those for the corresponding compression loading. This means that in such situations many negative eigenvalues (corresponding to compressive loading) with absolute values smaller than for tensile loading would be calculated before the first positive eigenvalue (for tensile loading) appeared. In order to avoid computing at first the negative eigenvalues, a modification of the formulation of the eigenvalue problem is performed.

The eigenvalue η_i is split into a prescribed portion κ and an unknown portion γ_i. Thus, Eq. (3) reads now

$$(\mathbf{K}_0 + (\kappa + \gamma_i)\mathbf{K}_{lin}(\lambda = 1))\phi_i = \mathbf{0}\ , \tag{6}$$

leading to the eigenvalue problem

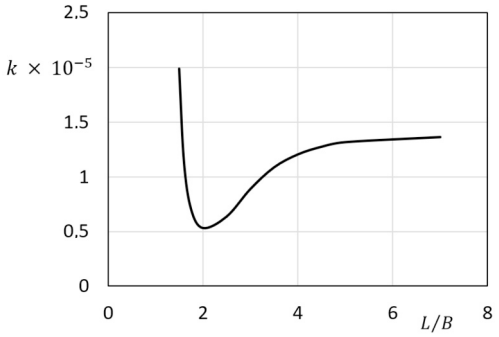

Fig. 2. Dependence of the buckling factor k on the L/B-ratio. As an example, the Poisson's ratio is chosen as $\nu = 0.3$.

$$(\tilde{\mathbf{K}} + \gamma_i \mathbf{K}_{lin}(\lambda = 1))\phi_i = \mathbf{0} \ , \ \text{with} \ \ \tilde{\mathbf{K}} = \mathbf{K}_0 + \kappa \mathbf{K}_{lin}(\lambda = 1) \ . \tag{7}$$

This way, the critical loads are given by

$$\mathbf{F}_i^* = (\kappa + \gamma_i)\mathbf{F}_{ref} \ . \tag{8}$$

Finally, the buckling load is given by

$$\mathbf{F}^* = \tilde{\lambda}^* \mathbf{F}_{ref} \ , \ \text{with} \ \ \tilde{\lambda}^* = \kappa + \gamma_1 \ . \tag{9}$$

The positive factor κ, which shifts the eigenvalues, must be chosen appropriately. There are some risks involved: If κ is too small, one gets negative eigenvalues, and if it is too large, the calculated smallest eigenvalue will lead to higher order buckling load, i.e., the fundamental buckling load is overlooked. Thus, the choice of proper values for κ requires careful checks.

It can easily be shown that the shift factor κ must fulfill the following inequality:

$$\frac{\tilde{\lambda}^* - |\lambda_1^-|}{2} \leq \kappa \leq \frac{\tilde{\lambda}^* + \kappa + \gamma_2}{2} \tag{10}$$

The use of the inequality Eq. (10) is not quite straightforward. In most cases the critical intensity for the corresponding compression loading, i.e., $|\lambda_1^-|$ can be calculated by known formulas or, if not, it can be simply determined by using Eq. (3), i.e., without any κ. However, γ_2 is not known in advance.

Since it is the absolute intention of this paper to present all results in dimensionless form, linearity has been assumed. On this basis, the PI-Theorem can be applied and for a given value of ν the dimensionless parameter

$$k = \frac{F^* B}{E t^3} \ , \tag{11}$$

is found, which is a function of L/B only. This parameter is frequently called "buckling factor".

3. Reconsideration and extensions - new observations

Using the above described procedure, parametric analyses (L/B is varied, ν is kept constant with $\nu = 0.3$) have led to results as presented in Fig. 2.

Fig. 2 corresponds quite well with the results presented in [1]. For large values of L/B, the here presented results are somewhat smaller than those in [1]. Furthermore, in [1] it is stated that for long strips ($L/B > 4.5$) the buckling factor becomes independent of its length. This statement will be reconsidered, too, and some unexpected results will be presented in the following chapters.

As mentioned above, the compressive stresses causing buckling of stretched strips results from hindering the Poisson's effect due to the boundary conditions. Thus, it is obvious that the value of the Poisson's ratio, ν, of the material, the strip is made of, must have a significant influence on the critical stretch force. It seems natural that an increasing ν leads to a decrease of the buckling force and, consequently, decreasing

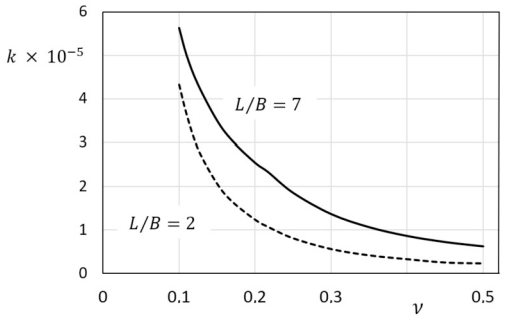

Fig. 3. Dependence of the buckling factor k on ν. The aspect ratio of the strip is chosen as $L/B = 2\ ,7$ as an example.

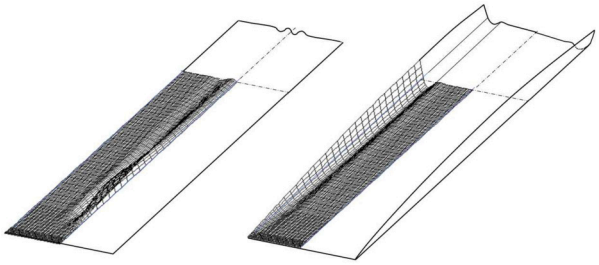

Fig. 4. Buckling mode before (left) and after (right) mode transformation, respectively. (Just a quarter of the strip is shown in detail.)

ν will increase this critical force. Against this background, the question arises as to whether buckling due to stretching of strips made of materials with a negative Poisson's ratio, i.e. auxetics, is even possible.

3.1. Variation of positive Poisson's ratios

As done in [1], let us distinguish between "short" and "long" strips. For instance, a strip with $L/B = 2$ is "short", and a strip with a ratio $L/B = 7$ or larger is typically "long".

From Fig. 2 one might expect that short strips behave principally different from long strips. Thus, the influence of the Poisson's ratio has been studied for strips with $L/B = 2$ and $L/B = 7$, respectively. The results of parametric studies are presented in Fig. 3 in terms of $k(\nu)$.

At first glance, nothing unexpected can be observed. However, when denoting the slight discontinuity of derivative of the function graph $k(\nu)$ for $L/B = 7$ in the range $\nu \approx 0.22$ one should ask for the reason of this.

A closer look at the buckling modes in this range of ν reveals that there appears a sudden, fundamental transition from modes with wrinkles in the area along the long axis (for $\nu > 0,22$) to modes showing uplifted strip edges (for $\nu < 0,22$), see Fig. 4.

Let us now consider if there is a significant difference in the character of $k(L/B)$ if the Poisson's ratio is varied, for instance, if ν is changed from 0.3 (as used in [1]) to 0.2.

Again, Fig. 5 shows nothing unexpected, and the above mentioned statement in [1], according to which for long strips $k(L/B)$ remains constant, seems to be valid. However, the above described observation of mode transition (see Fig. 4) makes clear: Caution is advised! And indeed, studying the behavior of the function $k(L/B)$ for $\nu = 0.2$ in more detail in the range $L/B = 7$ reveals a mode transition at $L/B \approx 6.6$, accompanied by a decline of the buckling factor with further increased L/B-ratios.

This phenomenon must be expected for all other ν-values with $0 < \nu \leq 0.5$, too. Fig. 7 represents a mode map, from which for given values of ν and L/B information can be obtained as to whether the stretched strip buckles with wrinkles parallel to the long axis or with uplifted edges.

Of course, when dealing with the problem of buckling of stretched strips, assuming only modes with folds parallel and close to the long

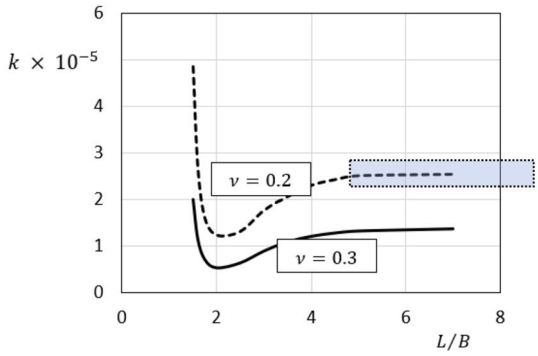

Fig. 5. Dependence of the buckling factor k on L/B for $\nu = 0.2$, 0.3. Both curves show principally the same character of the dependence of k on ν. The shaded box is considered in detail in Fig. 6.

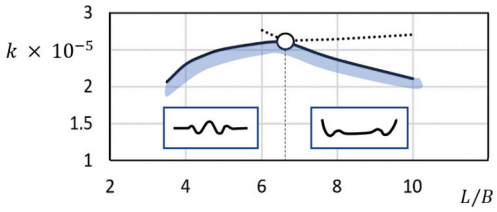

Fig. 6. Detail of Fig. 5 showing clearly the mode transition, which for strips with $\nu = 0.2$ appears at $L/B \approx 6.6$. For strips with other ν see Fig. 7.

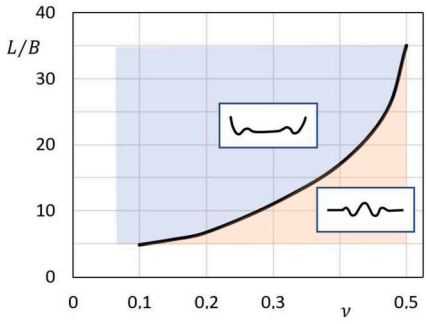

Fig. 7. Mode map, allowing the prediction of the buckling mode to be expected for given parameter combinations $(L/B\ , \nu)$ for $\nu > 0$. For $(L/B, \nu)$ combinations lying above the border curve, the buckling mode shows up or down bent long edges. Otherwise, wrinkles appear parallel to the long axis in the inner region of the strip.

axis of the strip (as mentioned in the Introduction), this mode transition cannot be found. Thus, results from such considerations should be considered with care, especially if long strips, made of materials with small, but still positive Poisson's ratios are concerned.

3.2. Extension to auxetics

Auxetic materials have negative Poisson's ratios. They are increasingly being used in technical, medical and sporting applications. In specific applications, their property of shrinking normal to the direction of a compressive load gives them some advantages over conventional materials, i.e., those with positive values of ν. A comprehensive description of auxetics can be found, e.g., in [42] or in [43]. Improving the buckling capacity of plates under compression by using auxetics is discussed in [44]. Medical applications are discussed in [45], and [46] as well as [47] provide insight into how auxetic materials are used in sports.

In [1] the appearance of transversal compressive stresses caused by the hindering of the Poisson's effect is clearly described for strips made

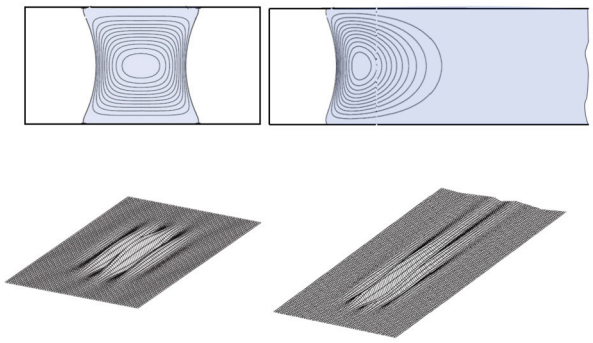

Fig. 8. Regions with transversal compressive stresses (shaded areas) and corresponding buckling modes, respectively, for stretched strips with $\nu > 0$. With the exception of the areas at the ends of the strip, the entire strip is subject to transverse compression, which of course varies in intensity.

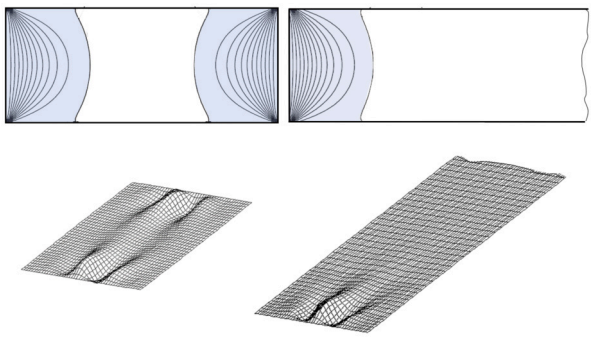

Fig. 9. Regions with transversal compressive stresses (shaded areas) for strips made of auxetics, i.e., $\nu < 0$. There, only the areas at the ends of the strip are subject to transverse compression, and the remaining portion is under transversal tensile stresses. Correspondingly, the wrinkles are concentrated in the end areas.

of material with $\nu > 0$. Fig. 8 shows for short and long strips the regions, in which these transversal compressive stresses appear (shaded areas).

As it is also shown in this figure, the regions and the distribution of the wrinkles correspond quite well with the location and distribution of the regions with transversal compressive stresses, at least as long as the wrinkle mode is concerned.

For auxetics, i.e., if the Poisson's ratio gets negative, the above described regions of transversal compressive stresses disappear, and instead transversal compressive stresses appear in regions directly at the ends of the strip, see Fig. 9. Correspondingly, if the stretch is strong enough to produce buckling, the buckling mode shows buckles also in the regions close to the strip ends only.

Parametric studies reveal that the dimensionless buckling factor k of strips made of auxetics is by two orders of magnitude smaller than for comparable strips made of material with positive Poisson's ratios, see Fig. 10 and the above Fig. 3. Because of the fact that for $\nu < 0$ the areas of transversal stresses are, in contrast to strips with $\nu > 0$, located near the short edges of the strip only, it is not surprising, that the dependency $k(\nu)$ is independent of L/B as long as $L/B > 2$, see Fig. 11. This is the reason, why in Fig. 10 just one curve is shown. However, as Fig. 11 shows, a strong decrease of k with decreasing L/B can be observed if L/B gets smaller than 2.

4. Discussion of the results and explanation of the new observations

In general, most of the results presented above appear as expected and their significance lies primarily in the dimensionless quantification of the critical states w.r.t. buckling. However, there are some phenomena which require a deeper consideration and explanation.

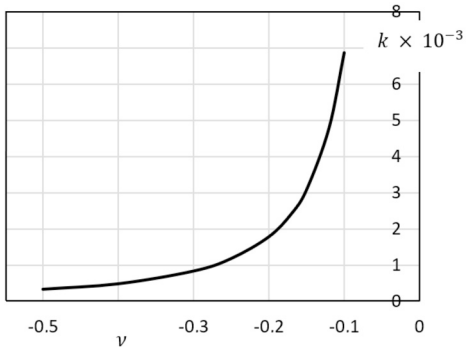

Fig. 10. Dependence of the buckling factor k on ν for stretched strips made of auxetic materials. For $L/B > 1.5$, this behavior is independent of the aspect ratio L/B. Thus, in contrast to Fig. 3, only one curve appears.

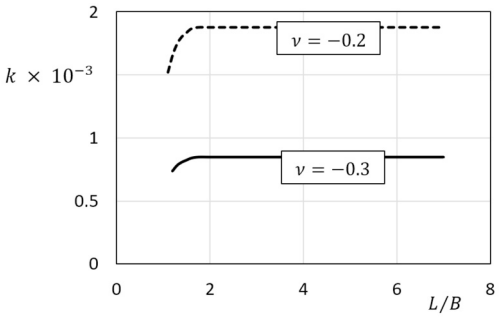

Fig. 11. Dependence of the buckling factor k on L/B for $\nu = -0.2$, -0.3, i.e., stretched strips made of auxetic materials. Note that for $L/B > 1.5$ the buckling factor k is independent of the aspect ratio of the strip.

4.1. Different reasons for the effect of the Poisson's ratio on k

In the Figs. 3 and 10 the dependency of k on ν is shown. Of course, the predominant reason for this strong dependency is the effect of hindered Poisson's deformations at the strip ends. The intensity of the transversal compressive stresses, caused by these boundary conditions, is directly proportional to ν. However, one might argue that also the bending stiffness K appearing in the Foeppl-v.Karman plate equation for pure in-plane loading

$$K\Delta\Delta w - t(\sigma_{xx}\frac{\partial^2 w}{\partial x^2} + \sigma_{yy}\frac{\partial^2 w}{\partial y^2} + \sigma_{xy}\frac{\partial^2 w}{\partial x \partial y}) = 0\,, \quad K = \frac{Et^3}{12(1-\nu^2)}\,, \qquad (12)$$

with

$$K = \frac{Et^3}{12(1-\nu^2)}\,, \qquad (13)$$

depends on the Poisson's ratio. By this way ν influences the buckling problem, too.

With Eq. (12), in classical configurations of plate buckling, i.e., with homogeneous stress fields, the dependence of the buckling factors on ν corresponds simply with the dependence of the plate's bending stiffness K on ν, leading to

$$\frac{k(\nu_1)}{k(\nu_2)} = \frac{1-\nu_2^2}{1-\nu_1^2}\,, \qquad (14)$$

where here $k(\nu_j)$ is the buckling factor of the plate made of material with $\nu = \nu_j$. Thus, for the mentioned simple classical cases (homogeneous tress fields) it is obvious that for $\nu > 0$ the buckling factor increases with increasing Poisson's ratio, and - since ν appears as ν^2 in Eq. (14) - the same happens for increasing absolute values of ν if $\nu < 0$.

In order to quantify and compare these two kinds of influences, i.e., hindered Poisson's deformations and varied bending stiffness, respectively, let us calculate the difference between $k(\nu_j)$ and $k_{\pm 0.3}$ in relation to $k_{\pm 0.3}$:

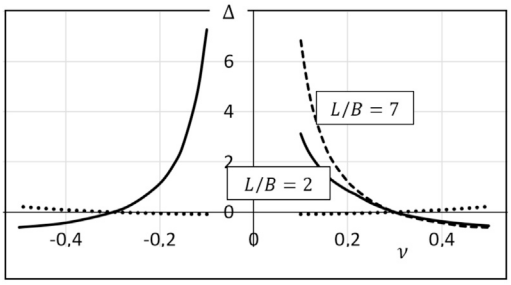

Fig. 12. Dependence of relative difference $\Delta(\nu)$ - see Eq. (15) - of the buckling factor k between those for the given value of ν and those for $\nu = \pm 0.3$. The contribution to Δ due to the influence of ν on the bending stiffness - see dotted line - is very weak compared to that caused by the influence of ν on the transverse compressive stresses responsible for wrinkle formation.

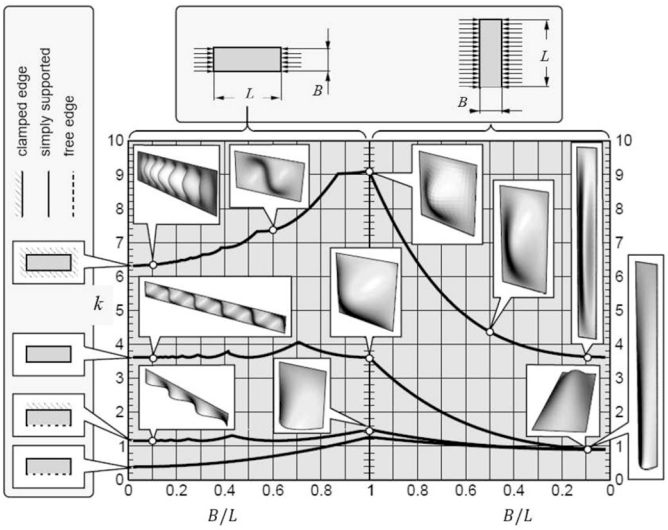

Fig. 13. Buckling factors for rectangular plates under homogeneously distributed edge loads. Plates with different boundary conditions are considered. k-values are valid for $\nu = 0.3$. Note that in the abscissa B/L but not L/B is varied. (Picture is taken from [48] with Wiley's permission.)

$$\Delta(\nu) = \frac{k(\nu) - k_{\pm 0.3}}{k_{\pm 0.3}}\,. \qquad (15)$$

In Eq. (15) the sign "+" stands for $\nu > 0$ and "−" for $\nu < 0$. This relative difference Δ is presented in Fig. 12. The dotted lines very close to the abscissa in the diagram represent the influence of the Poisson's ratio on k via the bending stiffness K. One clearly sees that this contribution is - in contrast to other configurations of stretched structures, as e.g. treated in [4] - negligibly small.

4.2. Dependence of k on L/B - positive ν-values

As Figs. 2 and 5 show, the buckling factor k depends for $\nu > 0$ strongly on L/B. Its minimum value is, within the considered range, at $L/B \approx 2$. It grows rapidly for smaller L/B-values. The increase of k for small L/B-values has two reasons. First, even for a homogeneous transversal compressive stress field the buckling factor increases strongly if L/B approaches 1, see Fig. 13. The second reason is that the region of transversal compressive stresses gets narrower if L/B gets smaller. This region is neighbored on both sides by regions of comparably strong transversal tensile stresses, which act like clamped boundaries.

For L/B-values growing from $L/B = 2$ further on, initially the buckling factor increases moderately. This is because the region of concentrated transversal compressive stresses becomes elongated and concentrated narrow. Thus, again, a narrower region of compressive stresses leads to an increase of k.

It seems that for $L/B > 6$ the buckling factor becomes constant. However, as already mentioned above, the impression of a constant k is deceptive. At a certain L/B-ratio, which depends on ν, a sudden mode transition happens from wrinkles in the area along the long axis to a buckling mode with uplifted (or down bent) long edges of the strip, accompanied by a reduction of the buckling factor when L/B is increased. This mode is caused by the fact, that for a long plate with a free edge the critical compressive stresses are very small compared to that for a long plate with both long edges clamped of simply supported, see Fig. 13. Looking at Fig. 8, one can see that the area of transverse compressive stresses continues - although with much smaller values - from the area of concentration stresses. Obviously, the effect of the free longitudinal edges outweighs the fact that the compressive stresses are larger in the concentration area.

Practical consequences of the appearance this (so far not detected) mode transition is that one must take into account that buckling in this mode appears at lower stretches than expected by the solutions assuming long wrinkles in the area long the mid axis of the strip, and measures for stiffening strips in order to avoid tensile buckling should take the possibility of such modes into account, too.

4.3. Dependence of k on L/B - negative ν-values

For strips made of auxetic material, buckling under longitudinal buckling is caused by transversal compressive stresses in the areas directly at the clamped short edges. Because these compressive stresses are much stronger than those occurring in the compressive stress concentration areas in strips made of material with positive ν, the buckling factors are much smaller, roughly by two orders of magnitude.

As Fig. 11 shows for $L/B > 2$, the bucking factor k is definitely constant. This is, why for these L/B-values the regions and values of the transversal compressive stresses and, thus, the deformation mode in the buckled areas remain all the same. Furthermore, since, except for the areas near the short edges, there is no other area of transversal compressive stresses (see Fig. 9), no mode transition is to be expected.

4.4. Finally, a note of caution

The considerations and results presented are based on the assumption of linearity. This means that small pre-buckling displacements (and rotations) and linear elastic (isotropic and homogeneous) material were assumed. In practical applications, the fulfillment of these assumptions should be carefully checked.

A conservative upper bound can be derived for the ratio t/B up to which a linear stability analysis is permissible. The derivation of this upper limit uses the fact that the transverse stresses caused by the stretching the strip are much smaller than longitudinal stresses, σ_{xx}. (Apart from the strip ends they are even orders of magnitude smaller.) Thus, for the following consideration a uniaxial stress state can be assumed. Let's also assume as an approximation that σ_{xx} is homogeneously distributed over the width of the strip.

Based on the above assumptions, Eq. (11) leads to the critical value of the longitudinal stress

$$\sigma^* = \frac{F^*}{B\,t} = kE\left(\frac{t}{B}\right)^2 . \tag{16}$$

With the above approximate assumptions the critical stretch is $\varepsilon^* = \frac{\sigma^*}{E} = k(\frac{t}{B})^2$. Let's accept that linear buckling analysis is permitted under the conditions that the pre-buckling strains must not be larger than an appropriately chosen value ε_{max}. Thus, the condition $\varepsilon^* < \varepsilon_{max}$ leads to the upper bound for $(\frac{t}{B})_{lim}$, which limits the ratio t/B, for which linear stability analysis can be applied:

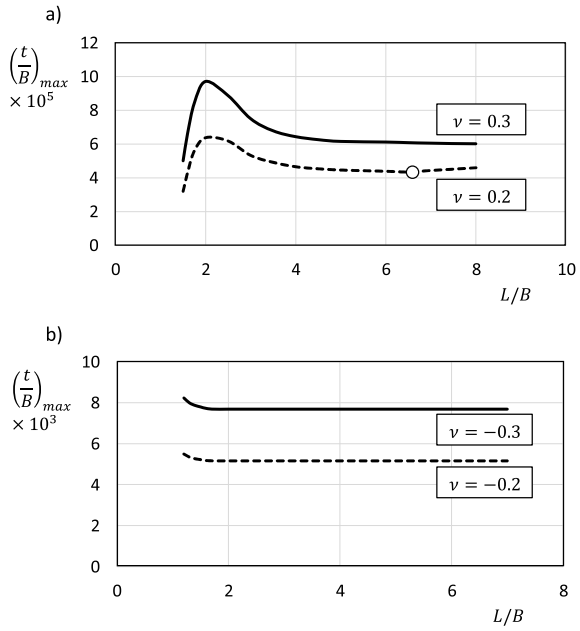

Fig. 14. Upper bounds for t/B up to which linear stability analysis is acceptable from a geometric point of view, i.e., prebuckling strains are smaller than, e.g., $\varepsilon_{max} = 0.05$, (a) for strips of material with positive Poisson ratios, $\nu = 0.2, 0.3$, (b) for strips of auxetic material, $\nu = -0.2, -0.3$. Note that for strips made of auxetics thicknesses are permitted, which are two orders of magnitude larger than those permitted for strips made of materials with positive values of ν.

$$\left(\frac{t}{B}\right)_{lim} = \sqrt{\frac{\varepsilon_{max}}{k}} . \tag{17}$$

Note that this upper limit is independent of the Young's modulus of the material the strip is made of. However, since k is a function of L/B and of ν this bound depends on the Poisson's ratio and the aspect ratio of the strip. As an example, such upper limits are shown in Fig. 14 when ε_{max} is chosen as 0.05.

Of course, in addition to checking the applicability of the linear stability analysis, it must also be proven whether the stress state in the strip is in the range of linear elastic material behavior. As is usual in global structural analysis, the very local theoretical stress singularities in the corners at the strip ends need not be taken into account.

5. Conclusions

This paper adds another small stone to the colorful mosaic that represents the wide field of instabilities of structures under tensile loading. Since the transverse compressive stresses that are the cause of the buckling of the stretched strips result from the hindered Poisson effect, it is clear that the value of the Poisson's ratio of the material from which the strips are made has a significant influence on the critical stretch. This is studied systematically for strips, i.e., aspect ratios $L/B > 1.0$ and for Poisson's ratios in the range $-0.5 \leq \nu \geq 0.5$. Hence, strips of auxetic material are also being investigated. Furthermore, it is shown that for long strips with $\nu > 0$ there is a transition of the buckling mode from folds in the interior of the strip parallel to the long axis to a mode that shows upward or downward curved length edges. The aspect ratio of the strip at which this mode transition occurs depends strongly on the value of ν, and no such transition has been found for strips made of auxetic materials.

All results are presented in dimensionless form. Therefore, as long as a linear elastic, isotropic material and the applicability of a linear buckling analysis can be assumed, the results can be used independently of actual geometric and material parameters. A simple check for the applicability of linear buckling analysis is provided, too.

Of course, there are still open questions in this area of structural mechanics, and it is evident that the above mentioned mosaic contains a number of areas waiting to be filled. In particular, the study of cukling of strips of auxetic materials should be intensified and more comprehensive analyses and tests with detailed discussion of the results should be carried out in the near future.

Declaration of competing interest

The authors declare the following financial interests/personal relationships which may be considered as potential competing interests:

Member of the editorial board of the Journal "Computers and Structures". FGR

Data availability

No data was used for the research described in the article.

Acknowledgement

The financial support of this investigation by ILFB-TUW under Project Nr. D317010-6001 as well as by the TU Wien for open access publication is gratefully acknowledged. Figures 1, 8, and 9 are based on Figs. 3, 5, and 7 of [1] with Elsevier's permission.

Appendix A. Supplementary material

Supplementary material related to this article can be found online at https://doi.org/10.1016/j.compstruc.2023.107193.

References

[1] Friedl N, Rammerstorfer FG, Fischer FD. Buckling of stretched strips. Comput Struct 2000;78:185–90. https://doi.org/10.1016/S0045-7949(00)00072-9.
[2] Durban D. Instability of an elastic circular plate subjected to nonuniform loads. AIAA J 1977;15:360–5. https://doi.org/10.2514/3.7329.
[3] Ayoub EF, Leissa AW. Free vibration and tension buckling of circular plates with diametral point forces. J Appl Mech 1990;57:995–9. https://doi.org/10.1115/1.2897673.
[4] Faghfouri S, Rammerstorfer FG. Buckling of stretched disks - with comparisons and extensions to auxetics. Int J Mech Sci 2022;213:106876. https://doi.org/10.1016/j.ijmecsci.2021.106876.
[5] Tomita Y, Shindo A. Onset and growth of wrinkles in thin square plates subjected to diagonal tension. Int J Mech Sci 1988;30:921. https://doi.org/10.1016/0020-7403(88)90074-4.
[6] Segedin RH, Collins IF, Segedin CM. The elastic wrinkling of rectangular sheets. Int J Mech Sci 1988;30:719–32. https://doi.org/10.1016/0020-7403(88)90037-9.
[7] Riks E, Rankin CC, Brogan FA. The buckling behavior of a central crack in a plate under tension. Eng Fract Mech 1992;43:529–48. https://doi.org/10.1016/0013-7944(92)90197-M.
[8] Shaw D, Huang YH. Buckling behavior of a central cracked thin plate under tension. Eng Fract Mech 1990;35:1019–27. https://doi.org/10.1016/0013-7944(90)90129-5.
[9] Gilabert A, Sibillot P, Sornette D, Vanneste C, Maugis D, Muttin F. Buckling instability and pattern around holes or cracks in thin plates under tensile load. Eur J Mech A, Solids 1992;11:68–89.
[10] Shimizu S, Yoshida S, Enomoto N. Buckling of plates with a hole under tension. Thin-Walled Struct 1991;12:35–49.
[11] Rammerstorfer FG. Buckling of elastic structures under tensile loads. Acta Mech 2018;229:881–900. https://doi.org/10.1007/s00707-017-2006-1.
[12] Rammerstorfer FG, Fischer FD, Friedl N. Buckling of free infinite strips under residual stresses and global tension. J Appl Mech 2001;68:399–404. https://doi.org/10.1115/1.1357519.
[13] Cerda E, Ravi-Chandar K, Mahadevan L. Thin film wrinkling of an elastic sheet under tension. Nature 2002;419:579–80. https://doi.org/10.1038/419579b.
[14] Jacques N, Potier-Ferry M. On mode localisation in tensile plate buckling. C R, Méc 2005;333:804–9. https://doi.org/10.1016/j.crme.2005.10.013.
[15] Puntel E, Deseri L, Fried E. Wrinkling of a stretched thin sheet. J Elast 2011;105:137–70. https://doi.org/10.1007/s10659-010-9290-5.
[16] Kim T-Y, Puntel E, Fried E. Numerical study of the wrinkling of a stretched thin sheet. Int J Solids Struct 2012;49:771–82. https://doi.org/10.1016/j.ijsolstr.2011.11.018.
[17] Silvestre N. Wrinkling of stretched thin sheets: is restrained Poisson's effect the sole cause? Eng Struct 2016;106:195–208. https://doi.org/10.1016/j.engstruct.2015.09.035.
[18] Martins AD, Silvestre N, Bebiano R. A new modal theory for wrinkling analysis of stretched membranes. Int J Mech Sci 2020;175. https://doi.org/10.1016/j.ijmecsci.2020.105519.
[19] Yang J, Huang W, Giunta G, Belouettar S, Hu H. The boundary effects on stretch-induced membrane wrinkling. Thin-Walled Struct 2020;154:106838. https://doi.org/10.1016/j.tws.2020.106838.
[20] Zhu J, Zhang X, Wierzbicki T. Stretch-induced wrinkling of highly orthotropic thin films. Int J Solids Struct 2018;139–140:238–40. https://doi.org/10.1016/j.ijsolstr.2018.02.005.
[21] Yang Y, Fu C, Xu F. A finite strain model predicts oblique wrinkles in stretched anisotropic films. Int J Eng Sci 2020;155:103354. https://doi.org/10.1016/j.ijengsci.2020.103354.
[22] Healey TJ, Li Q, Cheng RB. Wrinkling behavior of highly stretched rectangular elastic films via parametric global bifurcation. J Nonlinear Sci 2013;23:777–805. https://doi.org/10.1007/s00332-013-9168-3.
[23] Li Q, Healey TJ. Stability boundaries for wrinkling in highly stretched elastic sheets. J Mech Phys Solids 2016;97:260–74. https://doi.org/10.1016/j.jmps.2015.12.001.
[24] Sipos AA, Fehér E. Disappearance of stretch-induced wrinkles of thin sheets: a study of orthotropic films. Int J Solids Struct 2016;97–98:275–83. https://doi.org/10.1016/j.ijsolstr.2016.07.021.
[25] Nayyar V, Ravi-Chandar K, Huang R. Stretch-induced stress patterns and wrinkles in hyperelastic thin sheets. Int J Solids Struct 2011;48:3471–83. https://doi.org/10.1016/j.ijsolstr.2011.09.004.
[26] Nayyar V, Ravi-Chandar K, Huang R. Stretch-induced wrinkling of polyethylene thin sheets: experiments and modeling. Int J Solids Struct 2014;51:1847–58. https://doi.org/10.1016/j.ijsolstr.2014.01.028.
[27] Wang T, Fu C, Xu F, Huo Y, Potier-Ferry M. On the wrinkling and restabilization of highly stretched sheets. Int J Eng Sci 2019;136:1–16. https://doi.org/10.1016/j.ijengsci.2018.12.002.
[28] Bonfanti A, Bhaskar A. Elastic stabilization of wrinkles in thin films by auxetic microstructure. Extreme Mech Lett 2019;33:100556. https://doi.org/10.1016/j.eml.2019.100556.
[29] Chopin J, Demery V, Davidovitch B. Roadmap to the morphological instabilities of a stretched twisted ribbon. J Elast 2015;119:137–89. https://doi.org/10.1007/s10659-014-9498-x.
[30] Kudrolli A, Chopin J. Tension-dependent transverse buckles and wrinkles in twisted elastic sheets. Proc R Soc A 2018. https://doi.org/10.1098/rspa.2018.0062.47420180062.
[31] Faghfouri S, Rammerstorfer FG. Mode transitions in buckling and post-buckling of stretched-twisted strips. Int J Non-Linear Mech 2020;127(103609):1–10. https://doi.org/10.1016/j.ijnonlinmec.2020.103609.
[32] Cordill MJ, Fischer FD, Rammerstorfer FG, Dehm G. Adhesion energies of Cr thin films on polyimide determined from buckling: experiment and model. Acta Mater 2010;58:5520–31. https://doi.org/10.1016/j.actamat.2010.06.032.
[33] Toth F, Rammerstorfer FG, Cordill MJ, Fischer FD. Detailed modelling of delamination buckling of thin films under global tension. Acta Mater 2013;61:2425–33. https://doi.org/10.1016/j.actamat.2013.01.014.
[34] Marx VM, Toth F, Wiesinger A, Berger J, Kirchlechner C, Cordill MJ, et al. The influence of a brittle Cr interlayer on the deformation behavior of thin Cu films on flexible substrates: experiment and model. Acta Mater 2015;89:278–89. https://doi.org/10.1016/j.actamat.2015.01.047.
[35] Fischer FD, Rammerstorfer FG, Friedl N, Wieser W. Buckling phenomena related to rolling and levelling of sheet metal. Int J Mech Sci 2000;42:1887–910. https://doi.org/10.1016/S0020-7403(99)00079-X.
[36] Jacques N, Elias A, Potier-Ferry M, Zahrouni H. Buckling and wrinkling during strip conveying in processing lines. J Mater Process Technol 2007;190:33–40. https://doi.org/10.1016/j.jmatprotec.2007.03.117.
[37] Huck WT. Artificial skins: hierarchical wrinkling. Nat Mater 2005;4:271–2.
[38] Li M, Zhu K, Qi G, Kang Z, Luo Y. Wrinkled and wrinkle-free membranes. Int J Eng Sci 2021;167:103526. https://doi.org/10.1016/j.ijengsci.2021.103526.
[39] Guo Z, Liu J, Yang S, Zhao W, Wang S, Ma Z. An in-situ low temperature-mechanical coupling test system for battery materials. IEEE Trans Instrum Meas 2023;72:6002309.
[40] Harris AK, Wild P, Stopak D. Silicone rubber substrata: a new wrinkle in the study of cell locomotion. Science, New Ser 1980;208:177–9.
[41] CARINA, Computer Aided Research in Nonlinear Analysis - the research FE tool of the Institute of Lightweight Design and Structural Biomechanics (ILSB), TU Wien.
[42] Yang W, Li Z-M, Shi W, Xi B-H, Yang M-B. Review on auxetic materials. J Mater Sci 2002;39:3269–79.
[43] Saxena KK, Das R, Calius EP. Three decades of auxetics research - materials with negative Poisson's ratio: a review. Adv Eng Mater 2016;18:1847–70.
[44] Zhang Y, Li X, Liu S. Enhancing buckling capacity of a rectangular plate under uniaxial compression by utilizing an auxetic material. Chin J Aeronaut 2016;29:945–51.
[45] Mardling P, Alderson A, Jordan-Mahy N, Le Maitre Ch Lyn. The use of auxetic materials in tissue enginering. Biomat Sci 2020;8:2074–83.
[46] Sanami M, Ravirala N, Alderson K, Alderson A. Auxetic materials in sport applications. Proc Eng 2014;72:453–8.

[47] Duncan O, Shepherd T, Moroney Ch, Foster L, Venkatraman PD, Winwood K, et al. Review of auxetic materials for sports applications: expanding options in comfort and protection. Appl Sci 2018;8:941. https://doi.org/10.3390/app8060941.

[48] Rammerstorfer FG, Daxner T. Berechnungs- und Design-Konzepte fuer den Leichtbau. In: Degischer HP, Lueftl S, editors. Leichtbau - Prinzipien, Werkstoffauswahl und Fertigungsvarianten. p. 14–49. Weinheim: Wiley-VCH. ISBN 978-3-527-32372-2, 2009.